Irradiation and Thermal Creep in UWCTR

P.A. Sanger

May 2, 1973

UWFDM-58

FUSION TECHNOLOGY INSTITUTE

UNIVERSITY OF WISCONSIN

MADISON WISCONSIN

Irradiation and Thermal Creep in UWCTR

P.A. Sanger

Fusion Technology Institute
University of Wisconsin
1500 Engineering Drive
Madison, WI 53706

http://fti.neep.wisc.edu

May 2, 1973

UWFDM-58

IRRADIATION AND THERMAL CREEP IN UWCTR

by

Phillip A. Sanger

May 2, 1973

FDM 58

I. Introduction

The phenomenon of radiation induced or enhanced creep in nonfissile materials received little attention before the discovery of void swelling in 1967[1] but since that time has been the subject of a program of investigation second only to the program directed toward void formation. The complexity of creep phenomena, the multitude of possible mechanisms and the expense associated with in reactor creep experiments however have delayed the formulation of a proven theory consistent with experimental data.

The high temperature service of most materials is limited to one-half the melting temperature largely by their thermal creep properties. Near this temperature, thermal creep rises dramatically and will determine the usefulness of the material as a structural member. In a nuclear reactor where normal operation temperatures are below 1/2 T_m, thermal creep is negligible but irradiation creep becomes important. Creep in the reactor context has a beneficial effect extending the serviceability of the material by relieving stresses built up from void swelling.

II. Thermal Creep

Creep is defined as a progressive plastic deformation with time under an applied stress. The general behavior of creep can be divided into three stages as shown in Figure 1.[2] Primary creep is characterized by the motion of mobile dislocations. The density of mobile dislocations steadily decreases due to pinning and dislocation pileups. In secondary

creep, an equilibrium density is reached and creep is produced by thermal activation of the dislocation past obstacles. The final stage, tertiary creep, is initiated by necking off and intergranular cracks.

Since thermal creep obviously involves thermally activated processes, it will be important to determine the temperature dependence of creep. It would be expected that this temperature dependence would reveal itself to be of the form exp - (ΔH_c/RT) where ΔH_c is the activation energy of the predominant creep mechanism. The creep of metals and and alloys is usually separated into low and high temperature behavior. Creep is believed to be governed by non-diffusion controlled mechanisms at low temperatures while at high temperatures, it is believed to be governed by diffusion-controlled mechanisms. From the experimental fact that high temperature creep involves self-diffusion, the temperature at which self-diffusion, and thus diffusion-controlled creep, becomes significant can be determined. The dependence of the coefficient of self-diffusion on temperature is given in equation 1. Empirically

$$D_s = D_o \exp\left(- \frac{\Delta H_s}{RT}\right) \qquad (1)$$

it has been found that $\Delta H_s \approx 38\ T_m$ where T_m is the absolute melting temperature[3] and ΔH_s is given in cal/mole/°K. A limiting temperature can be determined if self-diffusion is considered negligible for $D_s = 10^{-18}$ cm^2/sec.

$$\frac{T}{T_m} = \frac{38}{R \ln (D_o/D_s)} \approx .46 \qquad (2)$$

Thus, below half the melting point, the creep mechanisms will be non-diffusion controlled. The primary creep mechanism in this temperature range is cross slip. Intersection of dislocations and lattice friction are other possible mechanisms for low temperature creep but these play only a limited role in most metals.

Two diffusion controlled mechanisms play a dominant role in high temperature creep:[4] 1) Nabarro-Herring creep and 2) Weertman creep. Nabarro-Herring creep occurs viscously by a stress-directed diffusion of vacancies and is illustrated in Figure 2. Edge dislocations with their extra plane parallel to the stress will climb with the absorption of vacancies while edge dislocations perpendicular to the stress will climb with the emission of vacancies. The net effect is an elongation in the direction of the tensile stress. A key feature of Nabarro-Herring creep is that the creep strain is accomplished by a mass transfer of atoms.

The second major mechanism of high temperature creep involves the climb of dislocations around obstacles and the subsequent glide resulting in the creep elongation (Figure 3). The first step, that of climb, is rate controlling at high stresses. Weertman creep is dependent on dislocation climb as is Nabarro creep but, in the Weertman case, the direction of climb is not important whereas it is essential to the Nabarro mechanism.

The stress dependence of secondary creep will also be important to the development of design equations. A single function can be used to describe this stress dependence at both high and low stresses:[5]

$$\dot{\varepsilon}_s = A(\sinh \alpha\sigma)^n$$

Both A and α are temperature dependent. For low value of σ, this dependence reduces to a simple power dependence σ^n. The creep rate, $\dot{\varepsilon}$, takes the form $\exp(n\alpha\sigma)$ for high stresses. In Figure 4, this function is fitted to experimental data demonstrating the deviation resulting from the application of simple power and exponential fits over the whole range of stresses. The use of $(\sinh \alpha\sigma)^n$ is valid over all stress ranges.

The approach adopted to obtain design equations for nuclear reactors has been to fit general forms to experimental data. The exact form chosen varies from author to author but it practically always follows the general form

$$\dot{\varepsilon} = A \exp(- \Delta H_c/RT) \ (\sinh\alpha\sigma)^n$$

The particular case of the General Electric Design equation for 316 stainless steel in FTR is shown in Figure 5 as a function of 1/T at a stress of 10,000 psi.[6] The preliminary calculations for thermal creep in UWCTR will be obtained from this curve.

III. Irradiation Creep

The discovery of void swelling in stainless steel cladding materials brought forth the need to relieve the differential stresses developed by such swelling. It was then that the role of irradiation creep was brought into prominence. The effect of irradiation on creep could be imagined to have two conflicting results, one enhancing creep and the other inhibiting creep. Since irradiation increases the number of vacancies and interstitials in the matrix, the creep rate would be expected to be enhanced. On the other hand, these defects migrate

and form larger defect structures such as voids and loops serving as obstacles to dislocation movement and thereby decreasing creep. The explanation that can be given is that creep is enhanced at low fluences by the increased defect concentrations while the matrix is hardened by the formulation of large stable defect structures at high fluences decreasing creep.

The search for dynamic mechanisms leading to irradiation creep must be approached from two directions: 1) the enhancement of thermal creep mechanisms and 2) entirely new mechanisms characteristic to the interaction of nuclear radiation with the matrix. In an earlier section, it was determined that self-diffusion became important at approximately half the melting temperature. This temperature corresponds to an activation energy sufficient to both form a vacancy and promote its migration. In the irradiation case, it will only be necessary to provide the migration energy to realize significant diffusion since the vacancies already exist in the metal. The temperature that corresponds to this condition is approximately three-tenths the melting temperature. Reactor cladding normally will operate at or above this temperature in future fast reactors. The resulting effects on creep rate will be discussed in greater detail later in this paper.

A multitude of new creep mechanisms arising from irradiation have been postulated. These mechanisms have recently been reviewed in detail by Gilbert[7] and only a brief summary will be presented here. A complete summary of the equations describing each of the mechanisms is given in Table 1.

1) Spike Relaxation. Thermal spikes resulting from energetic particles allow the matrix to anneal itself thus relaxing elastic strains and preventing strain hardening (Figure 6).[8,9]

2) Irradiation Growth. This growth occurs in anisotropic materials as a result of the preferred orientation of the irradiation produced platelets and loops (Figure 7a).[10] Its occurrence in cold-worked cubic metals is due to the asymmetry of the deformation and the rotation of active glide planes toward the axis of deformation.[11] In polycrystalline materials, this growth can lead to the associated mechanism of yielding creep in which internal intergranular stresses may locally excede the yield stress of the material resulting in plastic deformation (Figure 7b).

3) Transient Irradiation-Induced Climb. This mechanism postulates the bowing of dislocations as a result of applied stress, dislocation energy and the supersaturation of irradiation-produced defects (Figure 8a).[12] According to Hesketh, equilibrium is established when the flow of vacancies and interstitials are equal.

4) Steady State Loop Orientation. This model presented by Hesketh considers depleted zones and defect clusters which collapse into dislocation loops(Figure 8b).[13,22] The effect of stress is to induce this collapse for smaller clusters than would otherwise be possible. This mechanism is relatively independent of temperature and is linear in stress and flux. The experimental data shown in Figure 9 indicates excellent agreement with the two preceding models of Hesketh.[14] It might be noted here that the parameter C in the steady state creep expression is temperature dependent and increases with decreasing temperature.[15]

Mathematically this dependence is given by McElroy et. al.[16] as

$$C \propto \exp(1.405 - .0027\ T)$$

5) Volume Creep. This mechanism is synonymous with stress-assisted swelling. At high temperatures where voids are formed, tensile stress reduces the effectiveness of the surface energy to suppress void growth.[17] At low temperatures, applied stress increases the attractive field of the dislocation for an interstitial and thus increases the number of vacancies which escape recombination increasing swelling. Both of these cases are shown in Figure 11.

6) Loop Unfaulting. The collapse of depleted zones into loops has already been considered as a possible mechanism for irradiation creep. The next mechanism involves the fate of these loops. In close-packed structures, these loops are faulted until a critical size is reached at which time unfaulting occurs. This critical size is attained by the absorption of defects at high temperatures. This growth may occur at a higher rate and a lower temperature due to the coalescence of smaller faulted loops. An unfaulted loop is then free to glide and thereby increase the creep rate.[18] This mechanism has been adopted by Harkness and Li in an analytical model describing creep.[19,25] Their result, shown in Figures 12 and 13, demonstrate the effect of temperature on this process. The increase of creep rate at 500°C is due to loop unfaulting while a dramatic plunge in creep rate at somewhat lower temperatures results from the immobility of medium size faulted loops and their effectiveness in blocking the motion of unfaulted loops.

The treatment of enhanced diffusion-controlled mechanisms has led to much controversy in the last few years. Many authors such as Hesketh[20,21] contend that all diffusion-controlled mechanisms will be unaffected by irradiation produced defects since interstitials and vacancies are created in equal numbers leading to no net climb. Nichols and others[4] contend that, while this statement is true of Nabarro creep, Weertman may indeed be enhanced by irradiation. In order for irradiation to enhance diffusion-controlled creep, the following four conditions must exist according to Nichols:[4]

1) The climb of the dislocation must lead to glide which provides the creep strain;

2) There must be an imbalance in the rate of absorption of irradiation-produced vacancies and interstitials by the dislocations;

3) In a metal, with approximately equal populations of dislocations, whose equilibrium concentrations of defects are driven in opposite directions by the applied stress, the creep rate will be independent of neutron flux below some critical flux; (see Nichols[4] for details)

4) In certain circumstances when only one type of dislocation is present and the defect equilibrium concentrations are all affected in the same way, the creep rate will increase continually with increasing flux if the dislocations favor climb by the absorption of the defect produced in excess.

The case for irradiation enhanced thermal creep is certainly not definitely settled but it seems possible that, in certain mechanisms,

irradiation produced defects may play an enhancing role.

A unified description of the stress dependence of several creep mechanisms has been presented by Nichols for the zirconium alloys.[23] Creep is depicted as a complex sum of mechanisms added to similar electrical conductances. Figure 14 illustrates this complex sequence of stress dependences. The parameter "n" denotes the power of the stress dependence of the mechanism. Since glide and climb mechanisms are a sequential process, these creep rates are in parallel instead of in series. The work of Fidleris (Figure 15) would seem to substantiate this stress behavior for the zirconium alloys.[24]

At the present time, most design equations for in-reactor creep utilize the transient and steady state creep mechanisms of Hesketh. The utilization of this model for creep does not indicate the verification of these mechanisms as the source of creep but only their use as a convenient form to follow in curve-fitting the experimental data. Figure 16 illustrates the creep rates obtained from the design equations of several authors as a function of fluence for 316 stainless steel at 10,000 psi.[6] Both the equations of WARD and GE are transient-steady state forms while the AI equation adopts the form presented by Gittus for dislocation bowing.[31]

IV. Application to UWCTR

In most cases creep has a detrimental effect on the use of materials at high temperature. Just the opposite effect is seen in a reactor as can be best illustrated by the results obtained for FFTF.

Figure 17 a, b, c illustrate the stresses that will be developed in the FFTF reactor.[26,27] The sequence of events, as foreseen by the designers, are as follows. At start-up, the radial flux gradients (Figure 17a) and the vertical coolant-temperature gradients produce a thermal stress on the fuel assembly resulting in bowing of the assembly when restrained in the core (Figure 17b curve A). The action of creep on the structure relieves this stress during operation but during shut-down the assembly will bow in the opposite direction due to the cooling thermal stresses (curve B). Later in the life of the assembly, void swelling will contribute an additional bowing stress to the assembly (curve C). Creep will attempt to relax this stress (curve D). Since creep rate increases with applied stress, the creep rate will increase with increasing swelling-induced stresses. This increase can be quite dramatic as has been found to be the case with the zirconium alloys.

These calculations were made postulating a form of the creep equation approximately that of the Westinghouse fit in Figure 16. In that equation, the dependence on stress was only linear whereas the work by Fidleris,[24] Nichols[23] and Gittus[31] on zirconium alloys would indicate a higher order dependence. Figure 17c shows the sensitivity of the net bowing on the magnitude of the creep equation assumed. The two divergent cases are certainly within the realm of present experimental error, which indicates the desperate need for further experimental investigation.

The determination of the effect of creep on the University of Wisconsin fusion reactor design will be carried out using the design

equations now in use for the design of FFTF. The GE design equation is a slowly varying function of temperature and encompasses the lower shaded area for the temperature range of 350-650°C. The Westinghouse equation, on the other hand, is independent of temperature in that same temperature range and is shown in the top curve. This curve will represent the maximum creep that might be expected and the lower bound is formed by the GE curve. The inner region can be thought of as an area of uncertainty. In the discussion that follows, the maximum creep will be assumed to be valid until further clarification is obtained from experiment.

The Westinghouse (WARD) equation can not be used directly in the UWCTR design since the energy spectrum on which this equation is based, that is EBR II, is significantly different from the UWCTR spectrum. In light of this difficulty, the assumption is made that creep can be directly related to the displacements per atom, or dpa, in the matrix due to the neutron fluence. A similar approach was used by McElroy et. al.[16] in correcting for the variations in energy spectrum of the different reactors in which creep data has been obtained. The displacement rate for EBR II has been determined by Doran using the energy spectrum at the center of the core and a displacement energy of 33 eV.[28] His calculations yield 7.03 dpa per 10^{22} n/cm^2. In the calculations reported by Kulcinski for stainless steel in UWCTR,[29] a displacement energy of 24 eV was used. Since the dpa value is inversely proportional to the displacement energy, the Doran value may be modified to reflect this difference and thus a dpa to fluence conversion factor of 9.66 UWCTR dpa per 10^{22} n/cm^2 (EBR II) must be used. The use of this conversion

factor permits the plotting of elongation versus dpa as shown in Figure 18.

It is convenient to convert dpa into intervals of time for various positions in the blanket. This can be done utilizing the mapping of dpa/year presented by Kulcinski and shown in Figure 19.[29] The combination of Figures 18 and 19 permits the designation of elongation values throughout the blanket. Thus, after twenty years, the first wall is expected to undergo an elongation of less than 2% at a constant stress of 10,000 psi and a temperature in the range of 350-650°C.

Without a stronger stress dependence in the creep equation, it can be seen that the void swelling in the first wall will quickly exceed the creep capabilities of the material.[34] It is therefore realistic to examine the effect of 650°C operation as a means of increasing the creep rate. Figure 20 shows the results of both irradiation creep and thermal creep. Notice that irradiation creep is only significant at short times and thermal creep is dominant at long times. The overall effect is to increase the net elongation to 10% in twenty years. The interpretation of these numbers must take into account the time to rupture for stainless steel in these conditions. Rupture life relations for in-reactor creep are very poorly known but approximations can be made from thermal creep data.[32] A rupture life of 10,000 hours can be estimated for thermal creep at 650°C in austenitic stainless at 10,000 psi. In this case, rupture would occur after slightly more than a year of operation with slightly less than 1% elongation. It must be stressed that this estimate is extremely approximate and should be used only until such time that experimental data is available. The possibility of

superplastic behavior due to irradiation creep as proposed by Nichols[33] may lead to a major alteration to this value. Present experimental work on zirconium alloys suggests this behavior but no definite statement may be made without further data. Watkins and Woods reported no detectable necking for a Zircaloy-2 sample at 325°C and a flux of 3×10^{13} n/cm^2/sec.[35] The test terminated at 10% elongation after 7,000 hours. Superplastic behavior is predicted to show 100% elongation. Unirradiated control samples exhibited necking at 2 to 3% elongation.

V. Conclusion

The results of this investigation into the effects of irradiation creep on the UWCTR design may be summarized as follows:

1) The stresses due to void swelling will exceed the creep induced relaxation unless creep is found to obey a higher stress dependance than the linear dependance predicted by Hesketh,

2) For the case of a first wall temperature of 650°C, thermal creep may increase the creep elongation by a factor of ten,

3) The elongation at the inception of tertiary creep will certainly exceed 10% and may be as great as 100% if in-reactor materials exhibit superplastic behavior. Therefore the rupture life will exceed the twenty year lifetime of the first wall,

4) Further experimental work must be carried out at higher fluences and various stress levels in order to validate one creep model over the others and to accurately determine the time to rupture of in-reactor components.

REFERENCES

1. C. Cawthorne and E. J. Fulton, "Voids in Irradiated Stainless Steel", Nature, 216,575 (1967).

2. F. Garofalo, Fundamentals of Creep and Creep-Rupture in Metals, MacMillan Co. (New York) 1965.

3. J. E. Dorn, "Creep and Fracture of Metals at High Temperature", NPL Symposium, London, HMSO, 89 (1956).

4. W. J. Duffin and F. A. Nichols, "The Effect of Irradiation on Diffusion-Controlled Creep Processes", J. Nucl. Mater., 45, 302 (1973).

5. F. Garofalo, "An Empirical Relation Defining the Stress Dependance of Minimum Creep Rate in Metals", Trans. AIME, 227, 351 (1963).

6. P. R. Huebotter, private communication.

7. E. R. Gilbert, "In-Reactor Creep of Reactor Materials", Reactor Technology, 14(3), 258 (1971).

8. J. A. Brinkman and H. Wiedersich, "Mechanisms of Radiation Damage in Reactor Materials", A.S.T.M. Spec. Tech. Pub. 380, 3 (1965).

9. J. S. Perrin, "Creep of Reactor Fuel Materials", BMI 1857, (1969).

10. R. V. Hesketh, "Nonlinear Growth in Zircaloy-4", J. Nucl. Mater.,

11. S. N. Buckley, "Irradiation Growth and Irradiation Enhanced Creep in FCC and BCC Metals", AERE-R-5944 (2), 547 (1968).

12. R. V. Hesketh, "A Transient Irradiation Creep in Non-Fissile Metals", Phil. Mag., 8, 1321 (1963).

13. R. V. Hesketh, "Irradiation Creep in Non-Fissile Metals", 10th Symposium on Special Metalurgy, "Brittleness and Irradiation Effects:, Saclay, France (June 23, 1966), CONF 660656, 185 (1967).

14. B. Watkins and D. S. Wood, "The Significance of Irradiation Induced Creep on Reactor Performance of a Zircaloy-2 Pressure Tube", ASTM-STP 458, 226 (1969).

15. E. R. Gilbert and L. B. Blackburn, "Irradiation Induced Creep in Austenitic Stainless Steels", Am. Soc. Metals 2nd. Int. Conf. on Strength of Metal and Alloys, (Aug. 30, 1970) Vol. 2, paper 9.9, 773.

16. W. N. McElroy, R. E. Dahl and E. R. Gilbert, "Neutron Energy Dependant Damage Function for Analysis of Austenitic Steel Creep Data", Nucl. Eng. Design, 14, 319 (1970).

17. E. R. Gilbert and J. L. Straalsund, "A Relationship for Non-conservative Volume Creep under Different States of Stress", Nucl. Eng. Design, 12, 421 (1970).

18. E. R. Gilbert and J. J. Holmes, "Irradiation Creep by Loop Unfaulting", Trans. Amer. Nucl. Soc., 13, 609 (1970).

19. S. D. Harkness, R. Grappel and S. G. McDonald, "SCIM, A Theory Based Computer Code for the Prediction of the In-Pile Behavior of 304 SS", HEDL-TME 72-64, page ANL-1.

20. R. V. Hesketh, "Diffusion Creep under Neutron Irradiation", J. Nucl. Mater., 29, 217 (1969).

21. R. V. Hesketh, "Dislocation Climb: First Catch Your Poisson", J. Nucl. Mater., 35, 253 (1970).

22. R. V. Hesketh, "Collapse of Vacancy Cascades to Dislocation Loops", Proc. Intern. Conf. Solid State Physics Research with Accelerators", BNL 50083 (C-52), 389 (1967).

23. R. A. Nichols, "On the Mechanisms of Irradiation Creep in Zirconium Base Alloys", J. Nucl . Mater., 37, 59 (1970).

24. V. Fidleris, "The Stress Dependance of the In-Reactor Creep Rate of Heat Treated Zr 2.5 w/o Nb and Cold-Worked Zircaloy-2", J. Nucl. Mater., 36, 343 (1970).

25. P. R. Huebotter, "Effects of Metal Swelling and Creep on Fast Reactor Design and Performance", Reactor Technology, 15 (2), 156 (1972).

26. R. J. Jackson, W. H. Sutherland and I. L. Metcalf, "Metal Swelling and Irradiation Creep Effects upon the Fast Test Reactor Core Component Performance:, BNWL 1430 (1970).

27. P. R. Huebotter, T. R. Bump, W. T. Sha, D. T. Eggen and P. J. Fulford, "Design, Research, Development Implications of Metal Swelling in Fast Reactors", ANL 7786 (1971)

28. D. G. Doran, HEDL-SA-482 (Aug. 1972), to be published.

29. G. L. Kulcinski, to be published.

30. M. A. Abdou,et al., "Preliminary Conceptual Design of a Tokamak Reactor", Paper to be published in Proc. of Texas Symp. on the Technology of Controlled Thermonuclear Fusion Experiments and the Engineering Aspects of Fusion Reactors November 1972.

31. J. H. Gittus, "The Theory of Dislocation Creep due to the Frenkel Defects or Interstitialcies Produced by Bombardment with Energetic Particles", Phil. Mag., 25, 345 (1972).

32. F. Garofalo, R. Whitmore, W. F. Domis and F. VonGemmingen, Trans. AIME, 221, 310 (1961).

33. F. A. Nichols, "Evidences for Enhanced Ductility during Irradiation Creep", Mater. Sci. Eng., 6, 167 (1970).

34. R. Brown, personal communication.

35. B. Watkins and D.S. Wood, "Significance of Irradiation Induced Creep on Reactor Performance of a Zircaloy-2 pressure Tube", ASTM-STP 458, 226 (1969).

Table 1 Mechanisms of Dynamic Irradiation Creep

reference 7

Equation No.	Author	Equation	Mechanism
5	Brinkman and Wiedersich[37]	$\epsilon_{sp} \simeq \epsilon_{el} V_{sp} \alpha_1 N_1 \chi_1 \phi t$	Spike relaxation
6	Perrin[40]	$\epsilon = \dot{\epsilon}^{p}_{th} t$	Spike annealing
8	Roberts and Cottrell[43]	$\dot{\epsilon} = \sigma \dot{\epsilon}_g / \sigma_y$	Yielding creep
9	Hesketh[51]	$\gamma = \tau/8\mu \, [1 - \exp(-\phi t/B)]$	Transient dislocation climb
10*a*	Hesketh[55]	$\dot{\epsilon} = C\sigma\phi$	Loop orientation (isotropic)
10*b*	Hesketh[39]	$\dot{\epsilon} \simeq A_3 \dot{\epsilon}_g \sigma / T$	Loop orientation (anisotropic)
11	Gilbert and Straalsund[64]	$\dot{\epsilon}_{mn} = \alpha(\phi,t,T)\sigma_{mn} + [\beta(\phi,t,T)W + \kappa(\phi,t,T)]\,\delta_{mn}$	Constant volume creep, volume creep, and swelling strain
14	McElroy, Dahl, and Gilbert[17]	$\bar{\epsilon}/\bar{\sigma} = 2 \times 10^{-9} \, [1 - \exp(-T\phi t)] + 4.5 \times 10^{-7} \, E\phi t \exp(1.14 - 0.0027T)$	Transient climb, loop orientation, and volume creep
16	Gilbert and Holmes[71]	$\dot{\epsilon} = b\pi(r_p^2 - r_c^2)\,\partial N_2/\partial(\phi t)\,\phi f(\sigma,T) + N_2 \pi r_p^2/\rho \, \dot{\epsilon}_{th}$	Loop unfaulting
17	Schoeck[73]	$\dot{\epsilon} = \dot{\epsilon}_{th}(1 + a^2 \alpha_2 \phi / D_{th} S_1)$	Dislocation climb enhanced by vacancy diffusion
18	Brinkman and Wiedersich[37]	$\dot{\epsilon} = \dot{\epsilon}_{th}(D_{th} + \dot{N}\,\overline{X^2})/D_{th}$	Dislocation climb enhanced by vacancy diffusion
19	Nichols[74,75]	$\dot{\epsilon} = A_5 \sigma^4 L^2 (D_{th} + \dot{N}\,\overline{X^2})$	Dislocation climb over obstacles enhanced by vacancy diffusion
21	Harkness, Tesk, and Li[20]	$\dot{\epsilon} = A_6 \sigma^2 L/\mu^2 bd \, (2D_{th}\sigma^2 bL/\mu kT + Q_{i,\mathrm{dis}} - Q_{v,\mathrm{dis}}/\mathrm{L}\,b^2)$	Dislocation climb over obstacles enhanced by interstitial diffusion
22	Nichols[25,74,75]	$\dot{\epsilon} = \dot{\epsilon}_g + \dot{\epsilon}_L + (1/\dot{\epsilon}_{\mathrm{int}} + 1/\dot{\epsilon}_{\mathrm{climb}} + \dot{\epsilon}_{\mathrm{cut}})^{-1}$	Composite mechanism: growth, loop orientation, glide, climb, and cutting
23	Ashby[97]	$\gamma = (N_i \Omega/\mu_R)\sigma\Omega$	Loop diffusion creep

Explanation of Symbols Used in Equations

ϵ_{sp} = strain induced by spikes
ϵ_{el} = elastic strain
V_{sp} = spike volume
α_1 = average number of spikes per neutron collision
N_1 = number of atoms per unit volume
χ_1 = neutron cross section per atom
ϕ = fast-neutron flux
t = time
ϵ = creep strain
$\dot{\epsilon}^{p}_{th}$ = primary stage of thermal creep
$\dot{\epsilon}$ = creep rate
σ = applied stress
$\dot{\epsilon}_g$ = growth strain rate
σ_y = yield stress
r_p = radius at which unfaulted loops are pinned
r_c = critical radius for loop unfaulting
N_2 = number of loops per unit volume
$\dot{\epsilon}_{th}$ = thermal-creep rate
ρ = dislocation density
D_{th} = thermal-diffusion coefficient
a = lattice parameter
α_2 = atom fraction of vacancies produced per unit fluence
S_1 = atomic fraction of places where vacancies and interstitials anneal out
$\dot{N}$ = atomic fraction of vacancies produced per time unit
$\overline{X^2}$ = mean-squared distance a vacancy must move to reach a sink
χ_2 = cross section for elastic collision with an atom
A_i = constant, where i = 1 to 6
T = absolute temperature, °K
C = irradiation-induced creep-rate coefficient
b = Burgers vector
$\dot{\epsilon}_{mn}$ = strain-rate tensor
σ_{mn} = stress tensor
α = coefficient to constant-volume irradiation creep
β = coefficient of the hydrostatic stress, W
κ = strain due to zero-stress swelling
$\bar{\epsilon}$ = effective strain for nonconservative volume creep
$\bar{\sigma}$ = effective stress
$\bar{E}$ = average neutron energy, MeV
δ_{mn} = Kronecker delta
L = spacing between obstacles
$D^* \simeq D_{th} + \dot{N}\overline{X^2}$
μ = elastic shear modulus
d = obstacle height
$Q_{i,\mathrm{dis}}$ = interstitial flux to dislocations
$Q_{v,\mathrm{dis}}$ = vacancy flux to dislocations
B = decay constant
$\gamma, \dot{\gamma}$ = shear strain and shear-strain rate
N_i = number of interstitials/(cm^3)(sec) absorbed by loops
μ_R = chemical potential of defects midway between dislocations
Ω = atomic volume of the defect

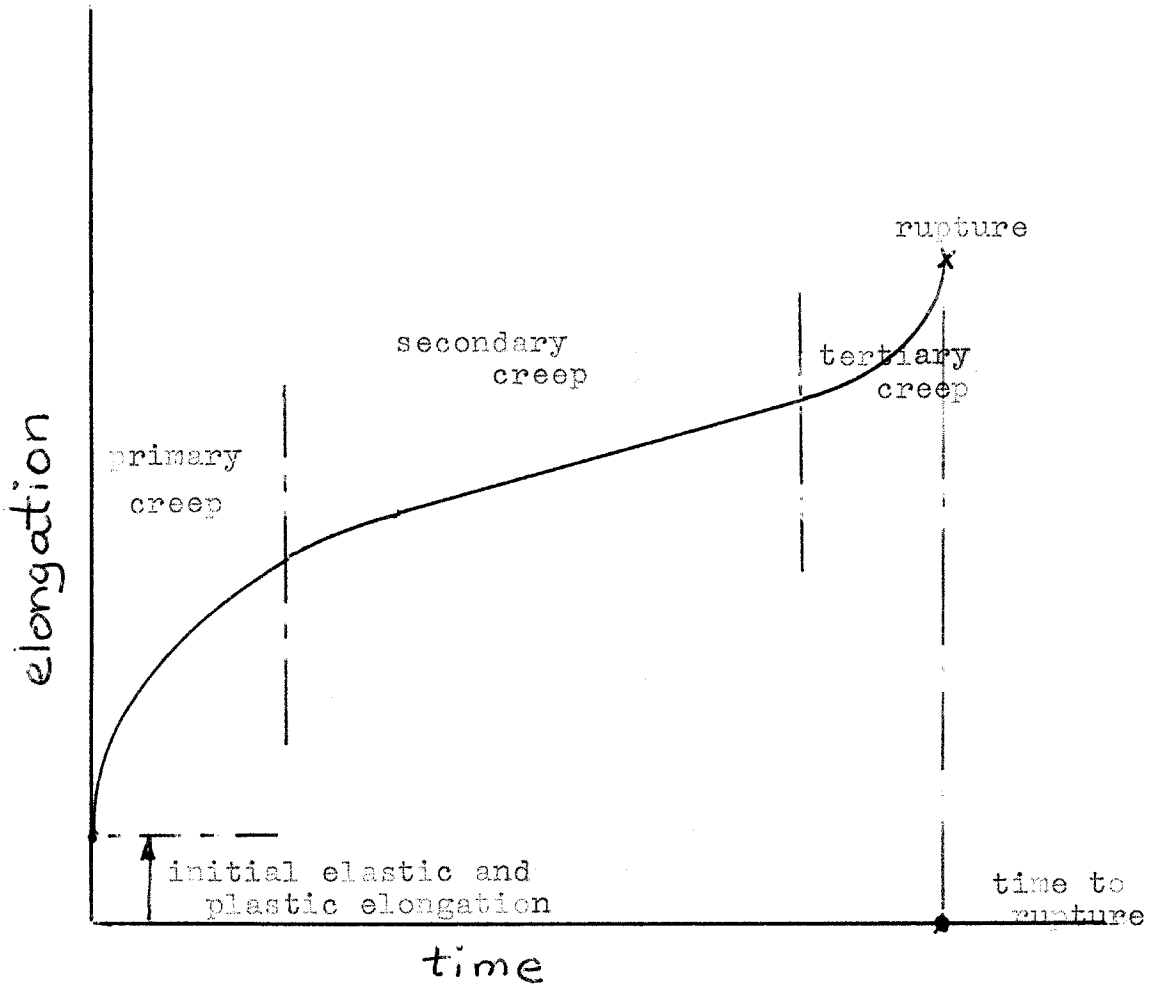

Figure 1. Typical creep behavior

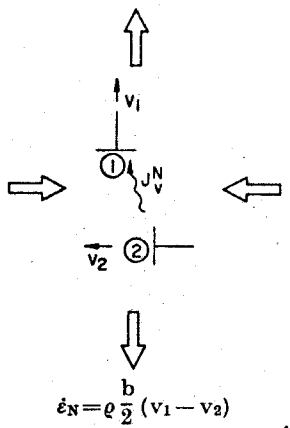

Fig. 2 Nabarro creep.

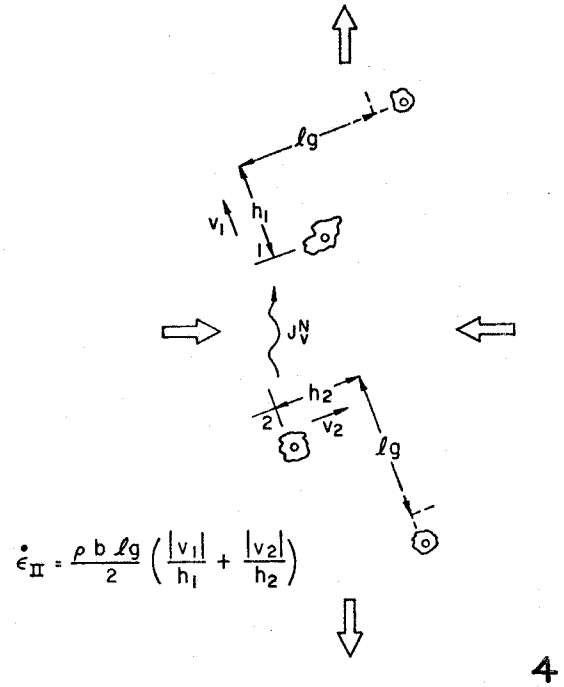

Fig. 3a Climb of interacting dislocations with glide.

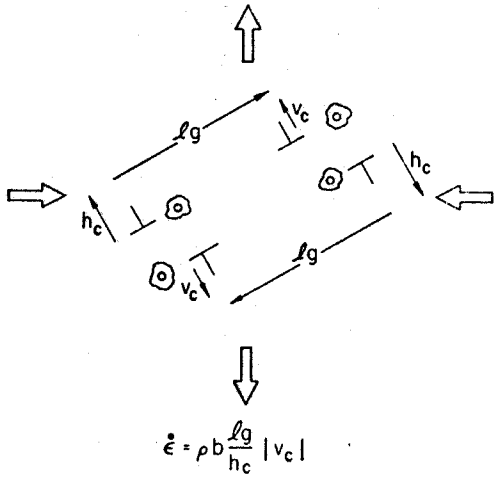

Fig. 3b Climb of non-interacting dislocations with glide.

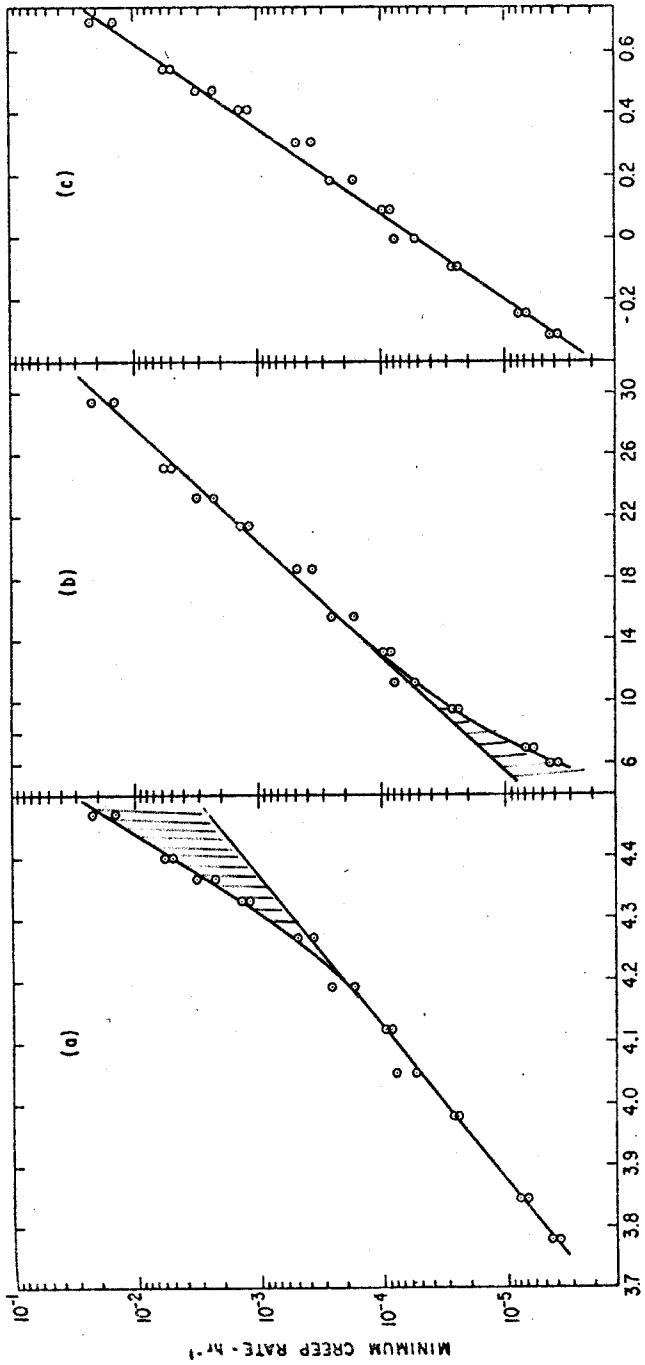

Fig. 4—Variation of log minimum creep rate with (*a*) log σ, (*b*) σ, and (*c*) log sinh ασ for 18 Cr-8 Ni-2 Mo austenitic stainless steel at 977°K (Ref. 10).

Reference 5

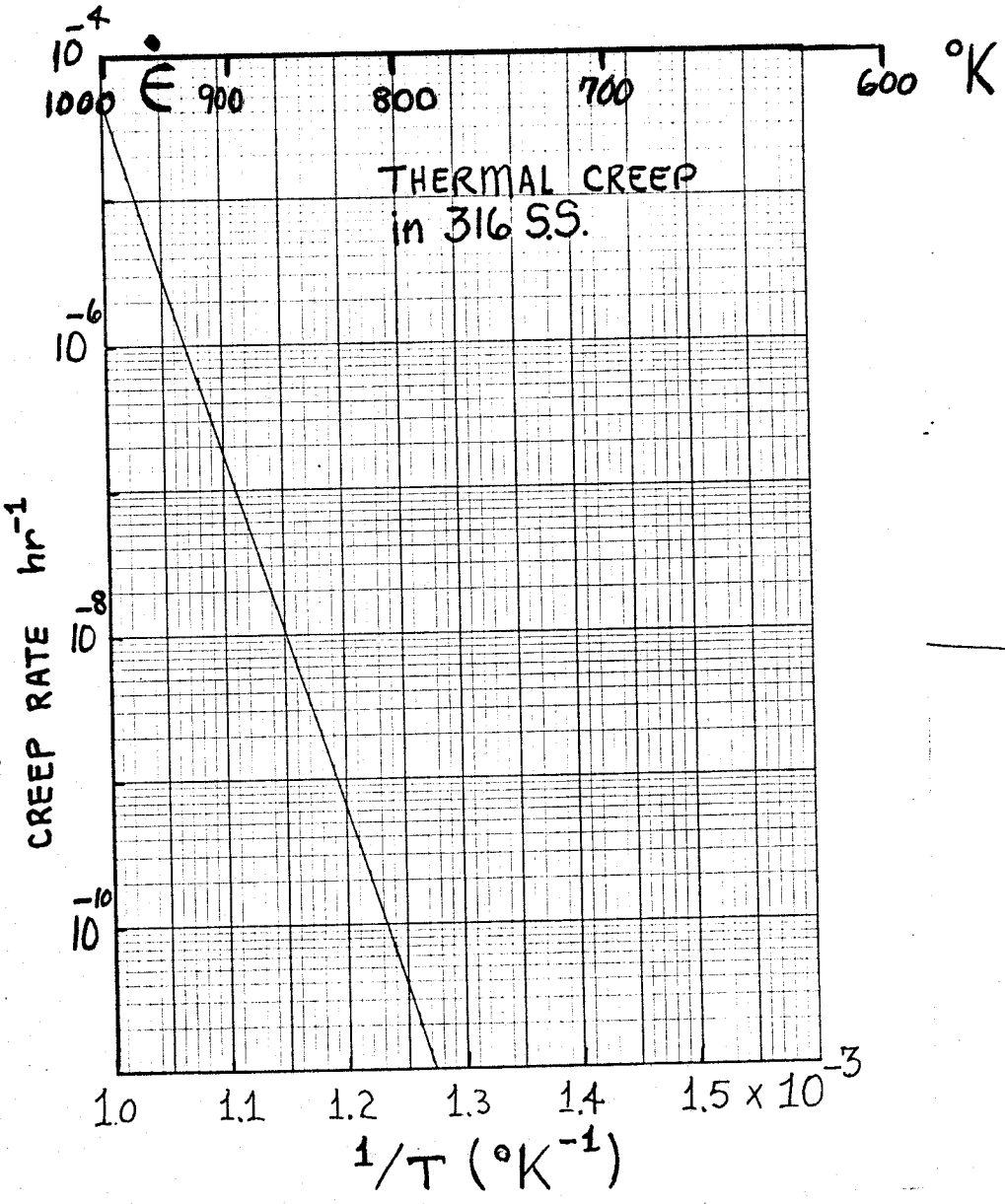

Figure 5. Thermal diffusion controlled creep at 10,000 psi according to the GE design equation.

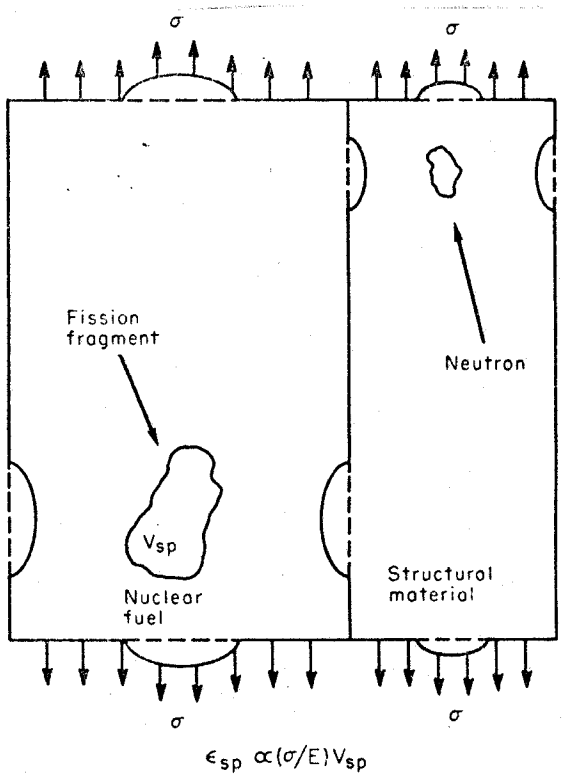

Fig. 6 Spike relaxation. Key: arrows indicate stress (sigma); solid lines indicate final specimen shape; broken lines indicate initial specimen shape. 7

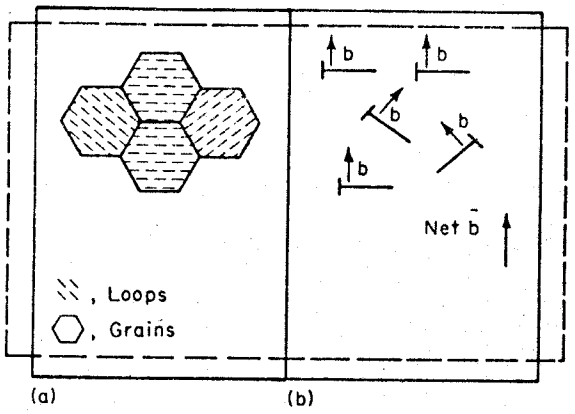

Fig. 7a Irradiation growth: (*a*) anisotropic material, (*b*) cold-worked isotropic material. 7

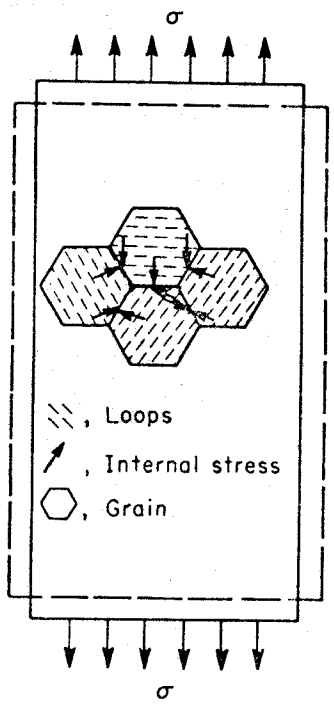

Fig. 7b Yielding creep. 7

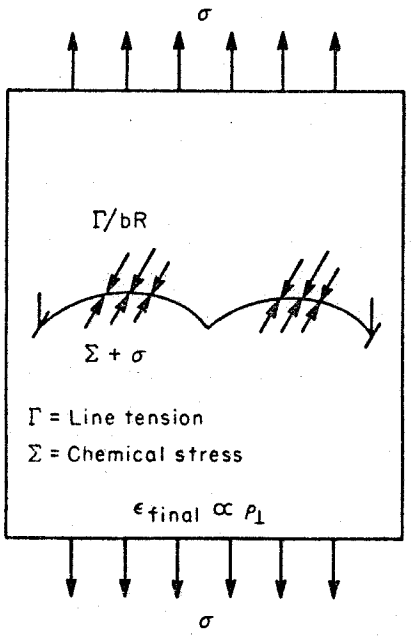

Fig. 8a Transient dislocation climb.

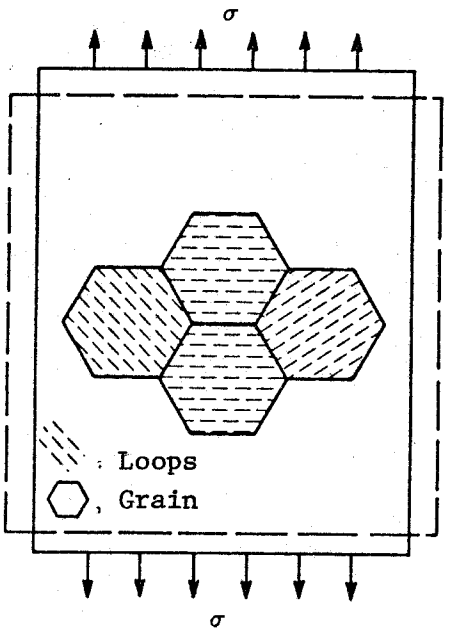

Fig. 8b Loop orientation.

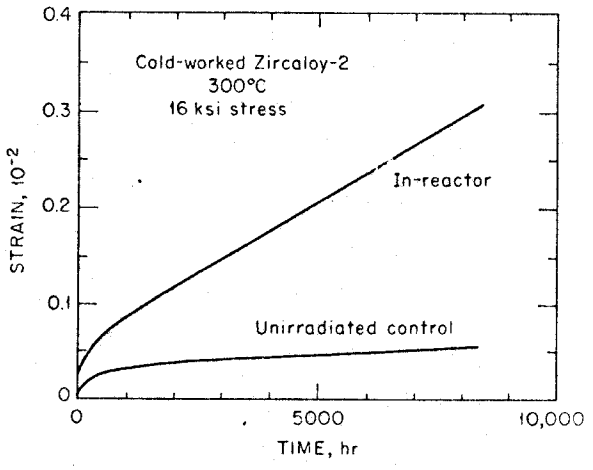

Fig. 9 Transient and steady-state irradiation creep in cold-worked Zircaloy-2.[22]

Reference 14

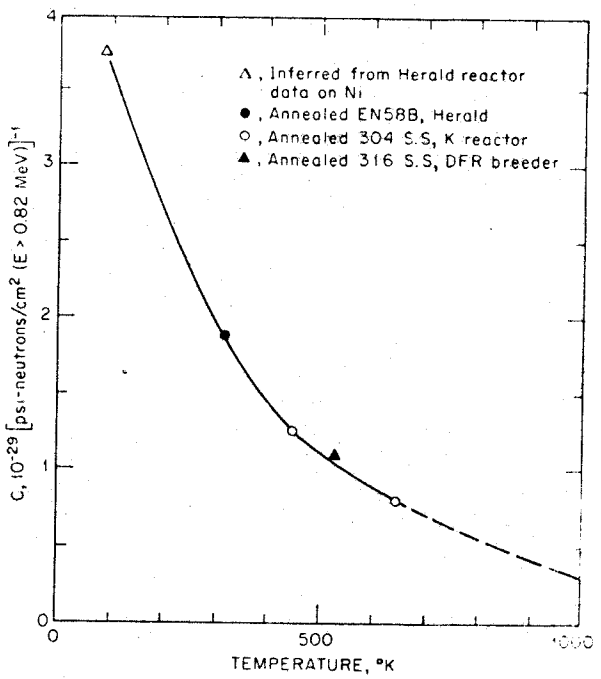

Fig. 10 Temperature dependence of the irradiation-induced creep-rate coefficient, C.[16]

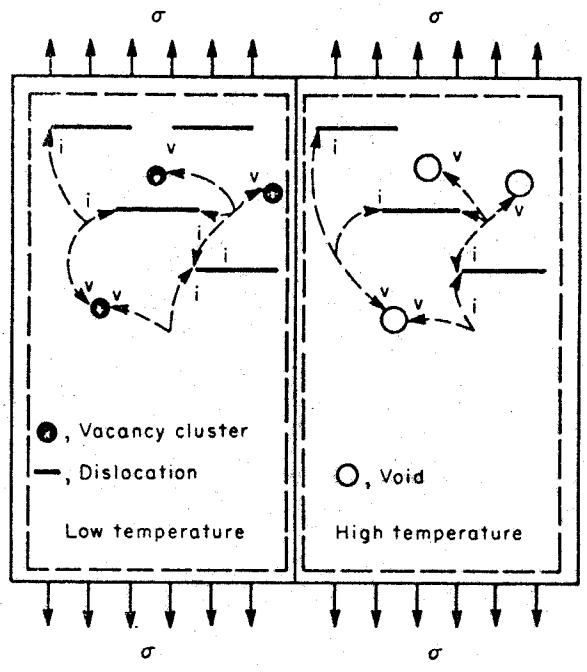

Fig. 11 Volume creep.[7]

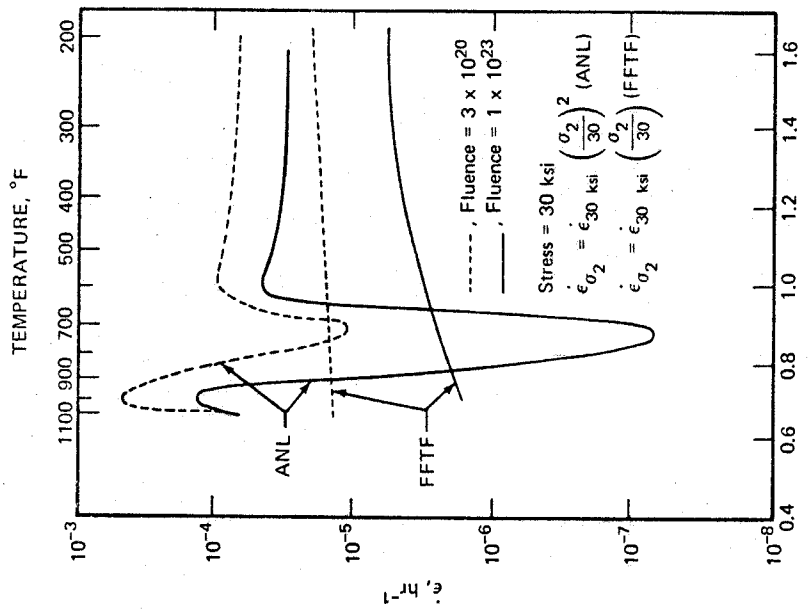

Fig. 13 Estimated radiation-enhanced creep rates from two different models.

25

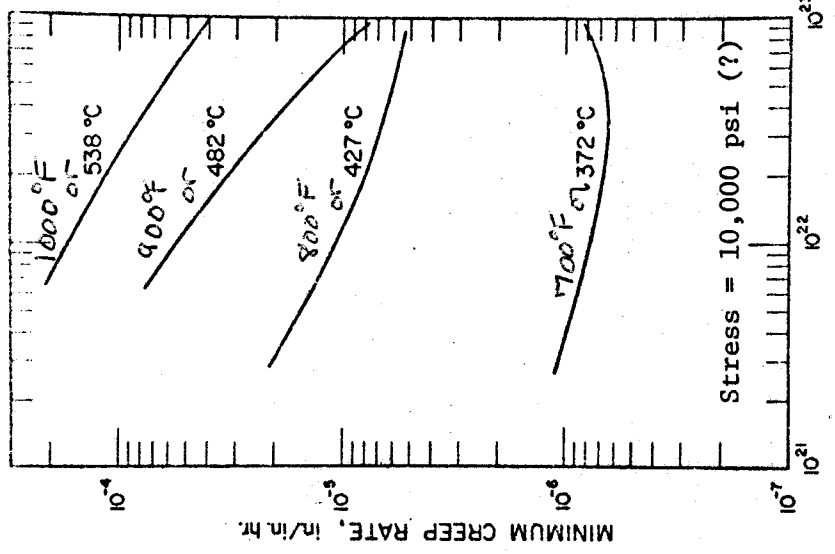

Figure 12
Predicted Effect of Neutron Exposure and Irradiation Temperature on In-Reactor Creep Rate

Reference 19

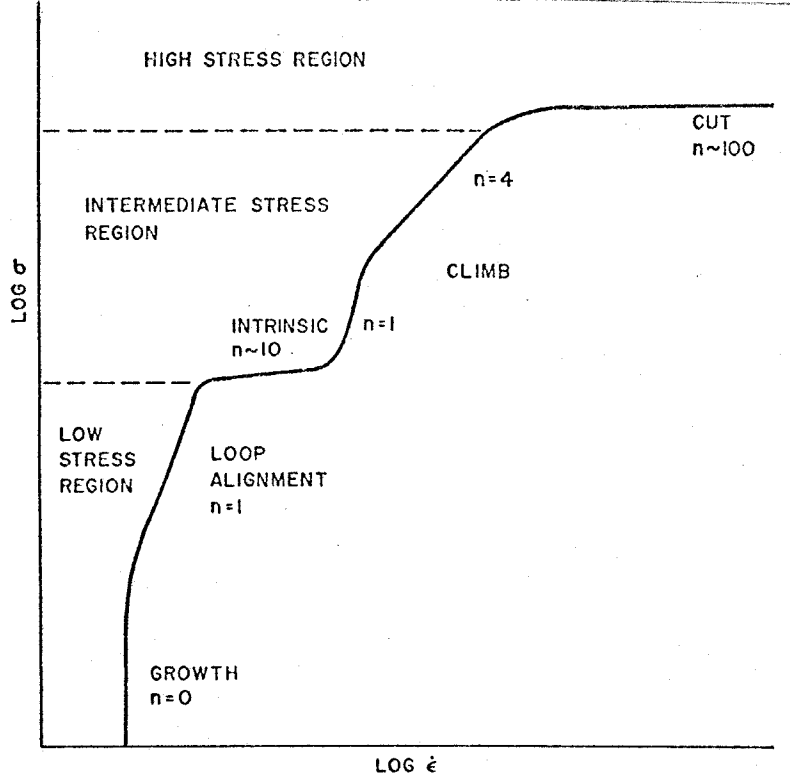

23

Fig. 14 Schematic representation of irradiation creep behavior of zirconium-base alloys.

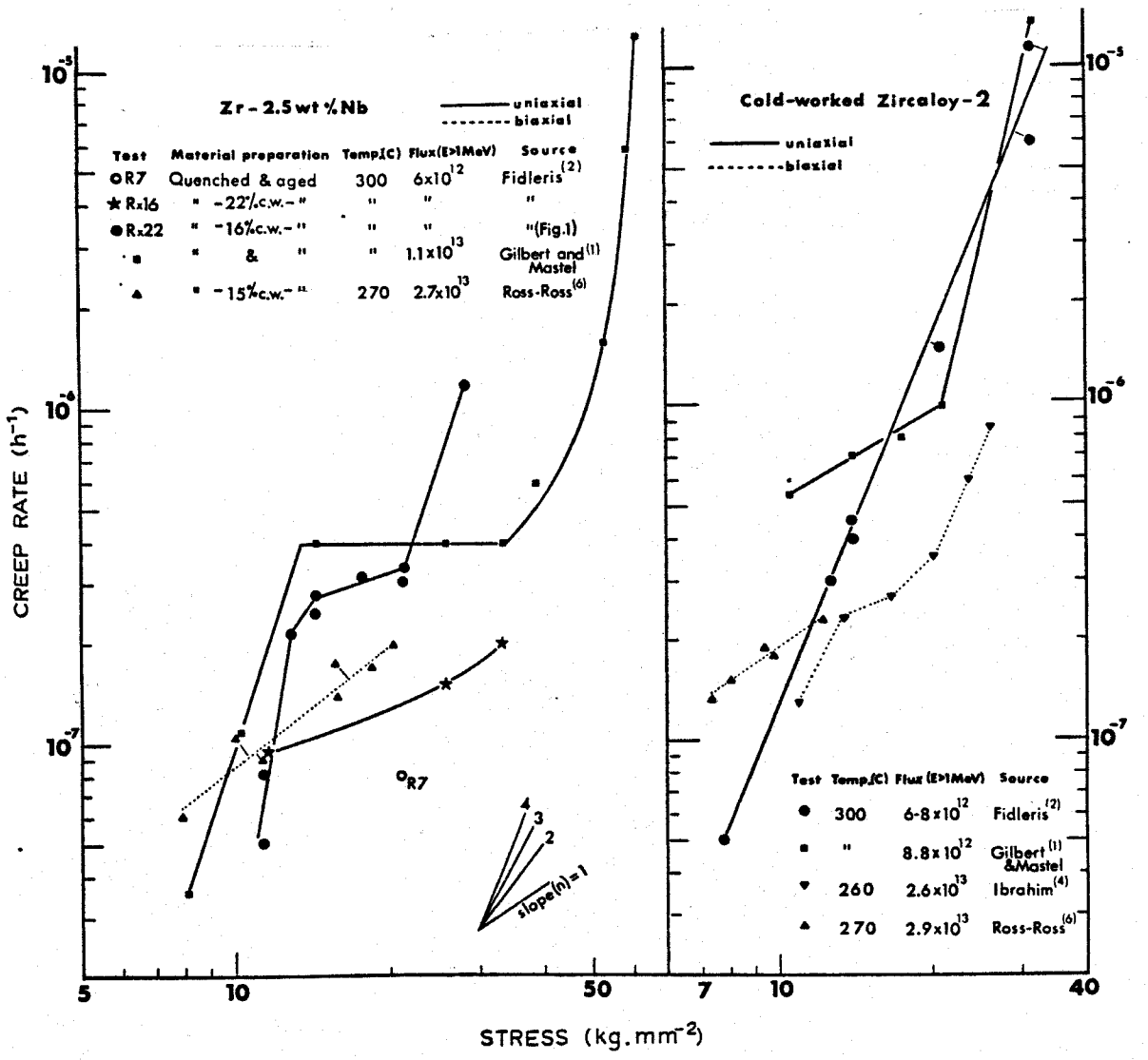

24

Fig. 15 Stress dependence of in-reactor creep rate of (a) heat treated Zr-2.5 wt % Nb; (b) cold-worked Zircaloy-2, during uniaxial and biaxial testing at 260–300 °C.

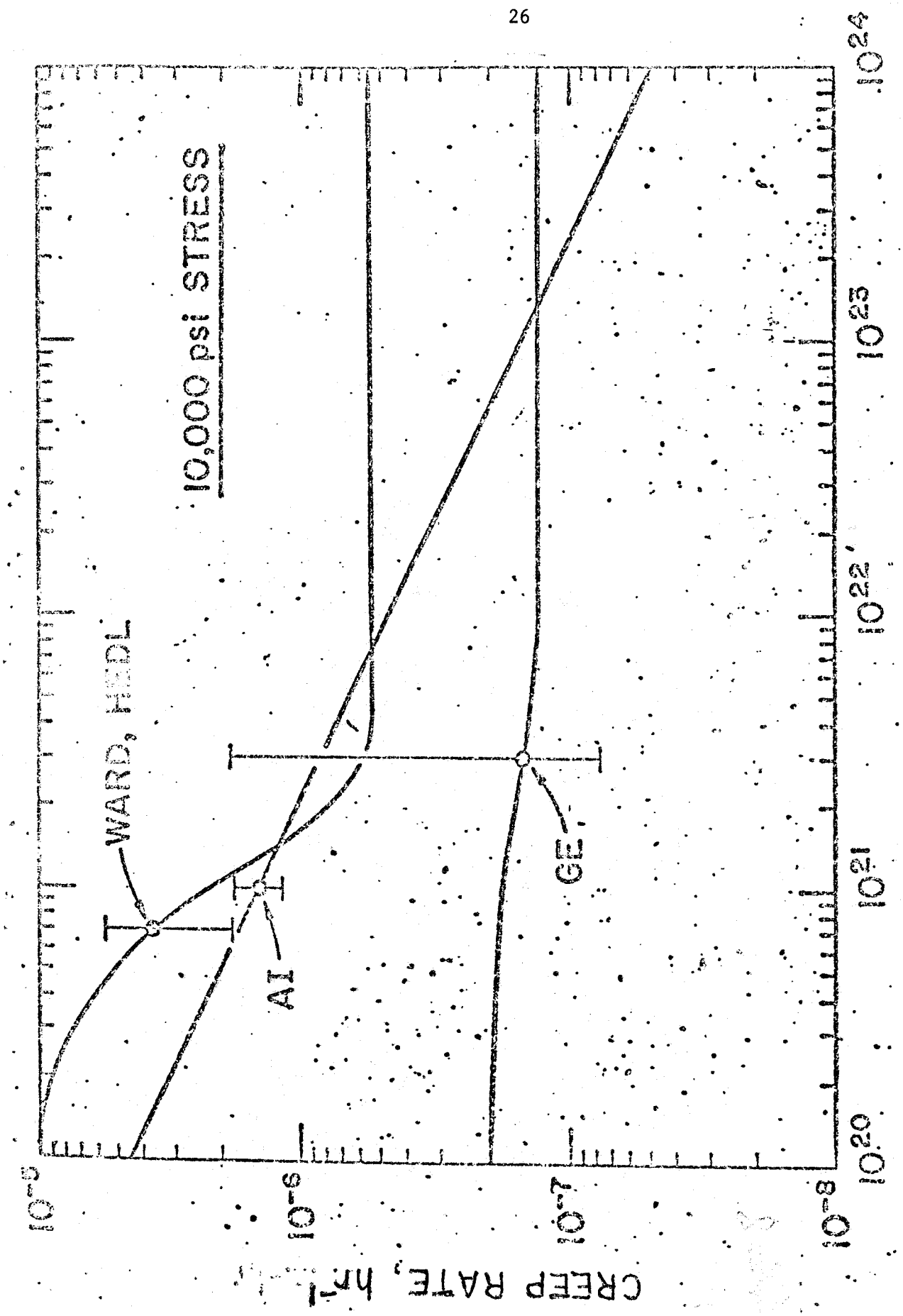

Fig. 16 Irradiation-induced Creep Rates at 900°F. Neg. No. ANL-306-1744

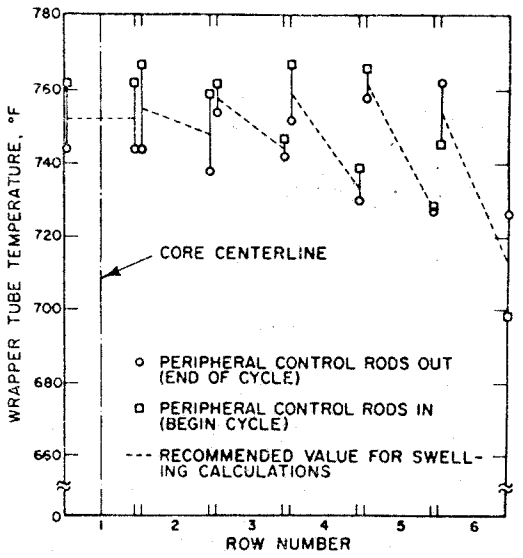

Fig. 17a Wrapper-tube Temperature 27 in. from Core Bottom. Neg. No. MSD-54148.

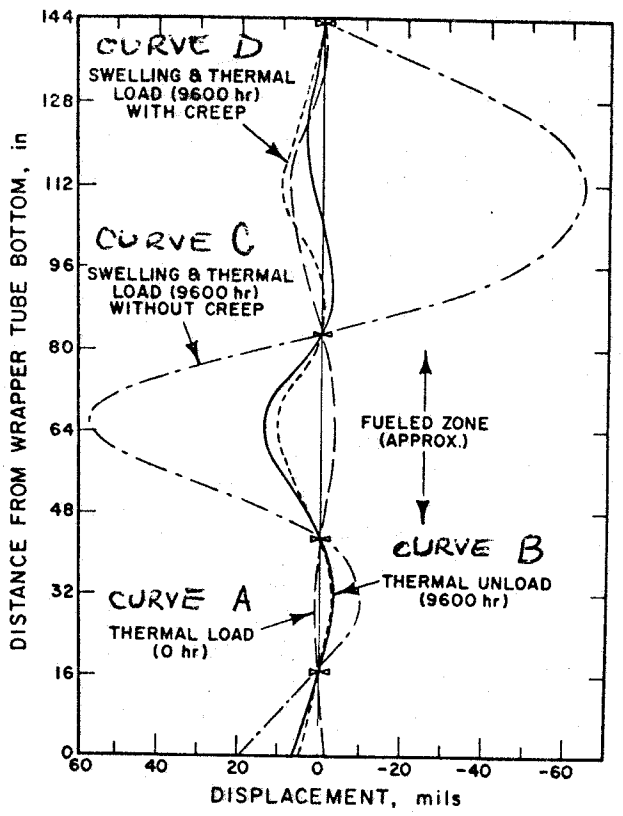

Fig. 17b Centerline Traverse of an Edge-core Assembly under Various Conditions. Neg. No. MSD-54411.

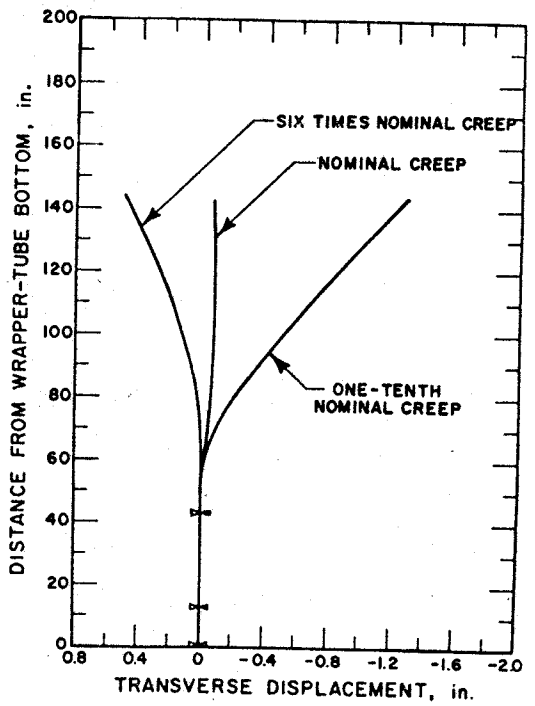

Fig. 17c Lateral Displacement of a Free Edge-core Assembly for Various Creep Equations. Neg. No. MSD-53596.

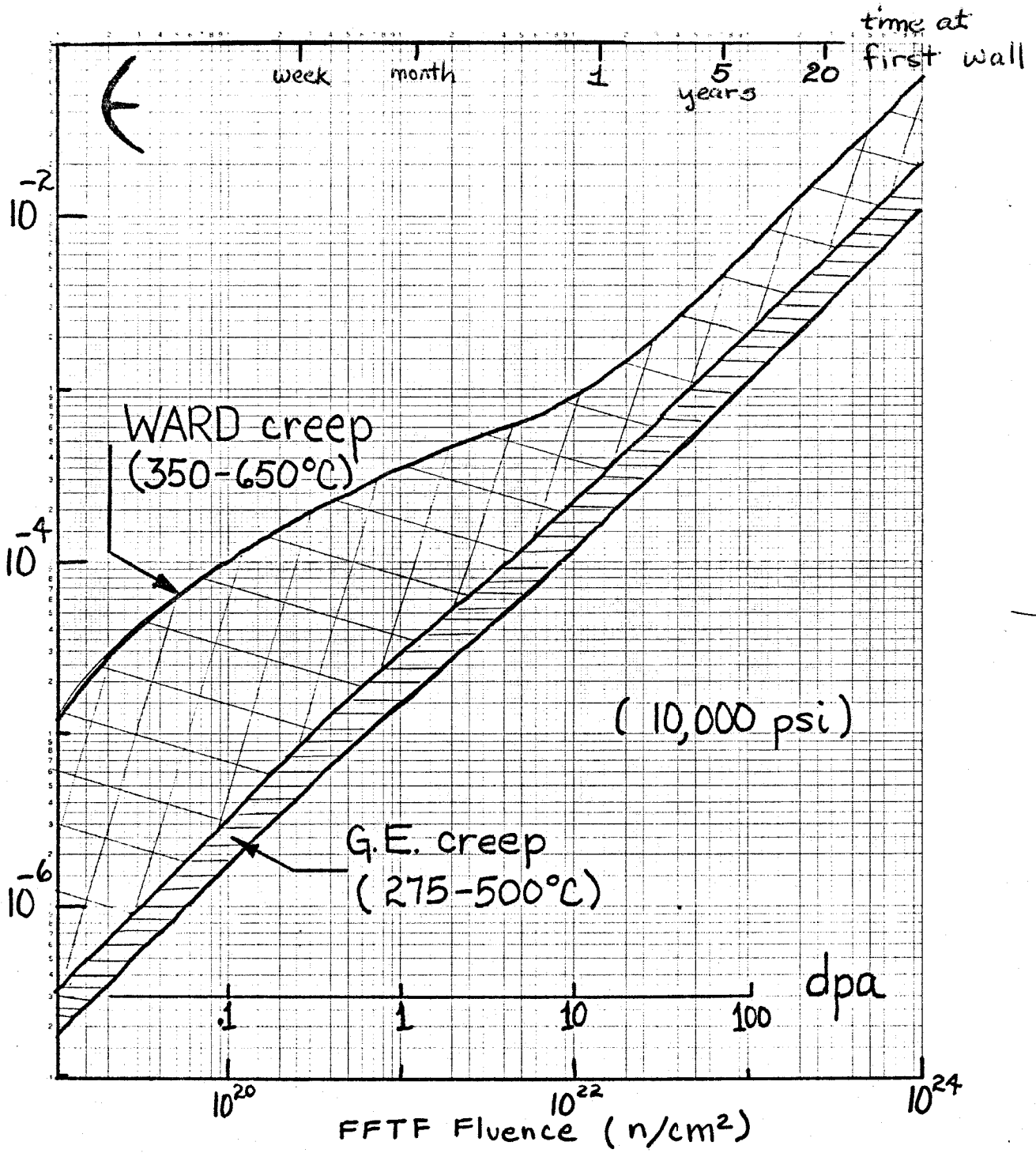

Figure 18 Elongation at 10,000psi in stainless steel versus FFTF Fluence. The conversion of 9.66 dpa per 10^{22} n/cm^2 has been used.

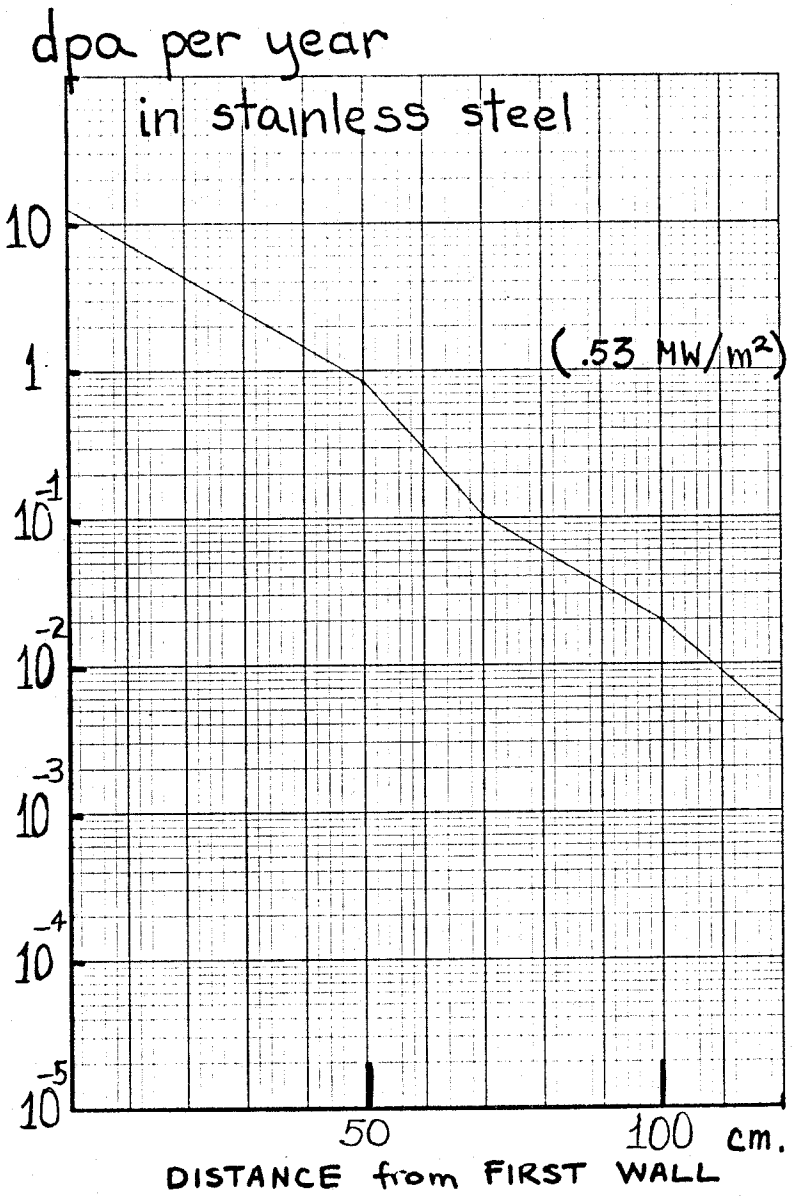

Figure 19. Mapping of the displacement damage as a function of the distance from the first wall.

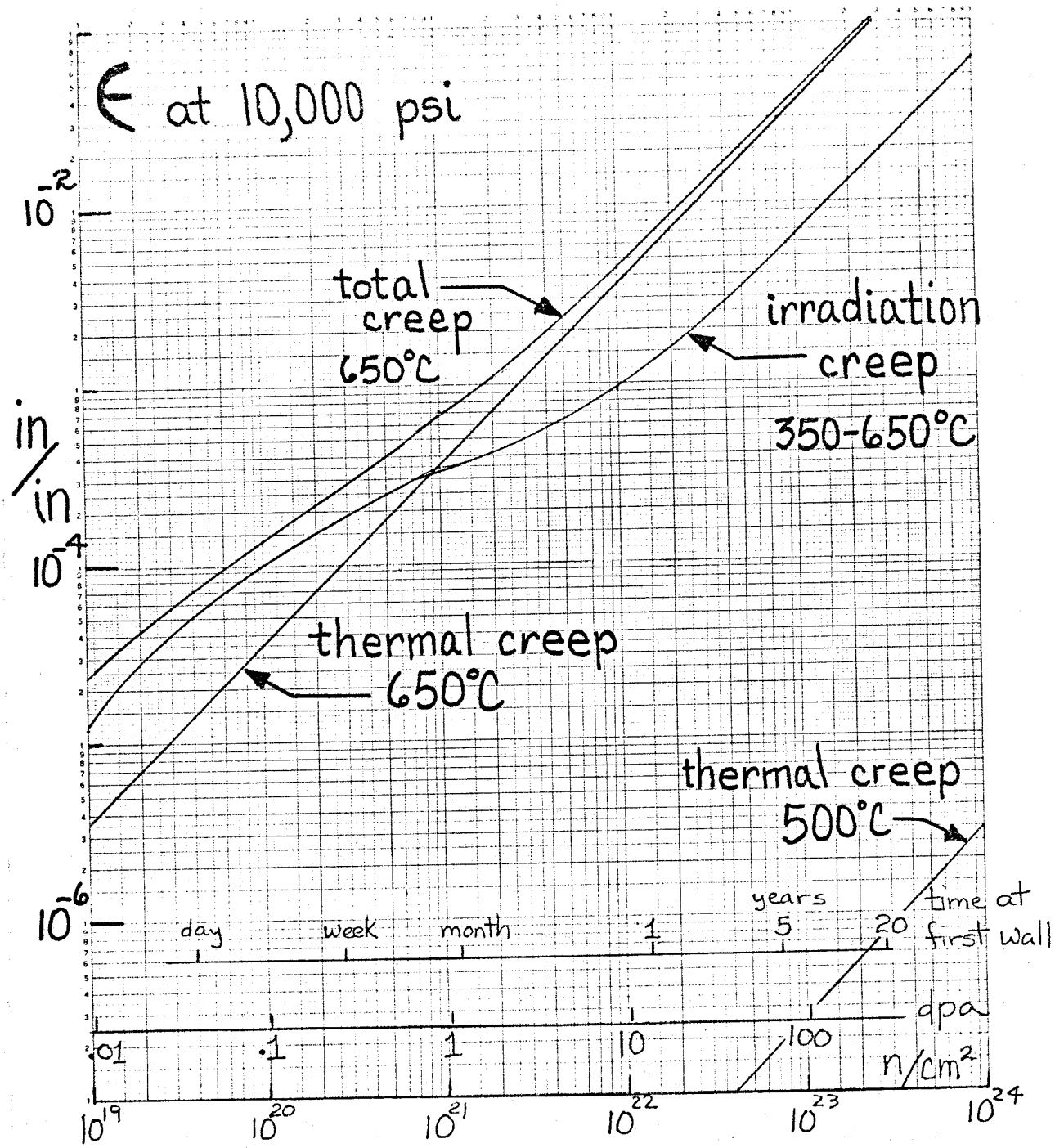

Figure 20. Elongation versus time at the first wall in UWCTR.